

Cite this: *Dalton Trans.*, 2019, **48**, 14000Received 30th July 2019,
Accepted 26th August 2019

DOI: 10.1039/c9dt03106e

rsc.li/dalton

Transforming PPh₃ into bidentate phosphine ligands at Ru–Zn heterobimetallic complexes†‡

Niall O'Leary, Fedor M. Miloserdov, * Mary F. Mahon* and Michael K. Whittlesey *

The reaction of [Ru(PPh₃)₃Cl₂] with excess ZnMe₂ led to P–C/C–H bond activation and P–C/C–C bond formation to generate a chelating diphenylphosphinobenzene ligand as well as a cyclometallated (diphenylphosphino)biphenyl group in the final product of the reaction, [Ru(dppbz)(PPh₂(biphenyl))(ZnMe)] (**1**; dppbz = 1,2-bis(diphenylphosphino)benzene); PPh₂(biphenyl)' = cyclometallated PPh₂(biphenyl). The mechanism of reaction was studied and C–C coupling to give a bidentate 2,2'-bis(diphenylphosphino)biphenyl (BIPHEP) ligand was suggested to be one of the key steps of the process. This was confirmed by the reaction of [Ru(BIPHEP)(PPh₃)HCl] with ZnMe₂, which also gave **1**. An analogous set of steps took place upon addition of ZnMe₂ to [Ru(*rac*-BINAP)(PPh₃)HCl] (*rac*-BINAP = racemic(2,2'-bis(diphenylphosphino)-1,1'-binaphthyl) to give [Ru(dppbz)(PPh₂(binaphthyl))(ZnMe)] (**3**). H₂ and the C–H bond of PhC≡CH added across the Ru–Zn bond of **1**, and also reversed the phosphine cyclometallation, to give [Ru(dppbz)(Ph₂P(biphenyl))(H)₂(H)(ZnMe)] (**4**) and [Ru(dppbz)(Ph₂P(biphenyl))(C≡CPh)₂(H)(ZnMe)] (**5**) respectively.

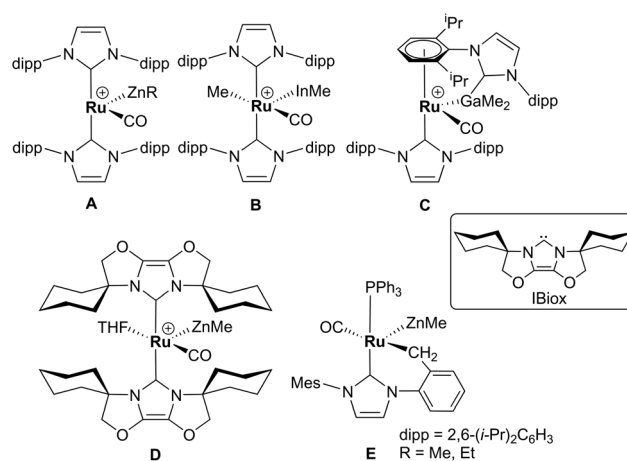
Introduction

Alkane elimination resulting from the treatment of a transition metal hydride (TM–H) complex with a main group hydrocarbyl (MG–R) reagent represents an established, but still under-utilised synthetic route to TM–MG heterobimetallic complexes.¹ We have recently employed this approach to good effect with ruthenium N-heterocyclic carbene (NHC) and/or phosphine hydride precursors and MG(alkyl)_{*n*} (*n* = 2, 3) compounds to generate a number of new Ru–MG (MG = Zn, In, Ga) complexes (Scheme 1).^{2–4}

With the cationic hydride precursors [Ru(NHC)₂(CO)H][BAR^F₄] (NHC = IPr, IBiox (see Scheme 1 for structures); [BAR^F₄] = [B(3,5-(F₃C)₂C₆H₃)₄], elimination of a single equivalent of C₂H₆ or CH₄ took place upon addition of ZnR₂ (R = Et, Me) to give [Ru(NHC)₂(CO)ZnR][BAR^F₄] (**A**, **D**).^{2,3} These complexes contain unsupported Ru–Zn bonds, which in the case of the IPr compounds, react readily with a range of E–H (E = H, B, Si) bonds. Addition of the group 13 trialkyls MMe₃

(M = Ga, In) to [Ru(IPr)₂(CO)H]⁺ resulted in chemistry that was different not only to that of ZnR₂, but also to each other. With InMe₃, methane loss was followed by methyl migration from In to Ru to generate [Ru(IPr)₂(CO)(InMe)Me][BAR^F₄] (**B**). With GaMe₃, a more complex set of reactions occurred that led ultimately to migration of an IPr ligand from Ru to Ga to yield **C**.⁴

The addition of excess ZnMe₂ to the neutral mixed NHC/phosphine precursor [Ru(IMes)(PPh₃)(CO)HCl] induced loss of two equivalents of CH₄, as well as ZnMeCl, to give the cyclometallated carbene complex [Ru(IMes)'(PPh₃)(CO)(ZnMe)]



Scheme 1 Examples of our recently reported Ru–MG heterobimetallic complexes. The [BAR^F₄] anion in each of the charged species has been omitted for clarity.

Department of Chemistry, University of Bath, Claverton Down, Bath BA2 7AY, UK.
E-mail: f.miloserdov@bath.ac.uk, m.f.mahon@bath.ac.uk,
m.k.whittlesey@bath.ac.uk

†MKW dedicates this paper to Professor Robin Perutz FRS on the occasion of his 70th birthday. Thank you Robin for the enthusiasm, guidance, encouragement and friendship over the last 30 years.

‡Electronic supplementary information (ESI) available. CCDC 1937663–1937665. For ESI and crystallographic data in CIF or other electronic format see DOI: 10.1039/c9dt03106e



E ((IMes)' = cyclometallated IMes).³ We have also established that the elimination of more than one equivalent of alkane is a feature of the reactions of $[\text{Ru}(\text{PPh}_3)_3\text{HCl}]$ with ZnMe_2 (as well as $\text{LiCH}_2\text{SiMe}_3$ and MgMe_2), the second equivalent of alkane now arising from Ru–H intermediates generated upon cyclometallation of a PPh_3 ligand.⁵ Given the wealth of Ru– PPh_3 precursors, we turned our attention to a non-hydride containing example to probe whether PPh_3 metalation still took place. Herein, we show that the reaction of $[\text{Ru}(\text{PPh}_3)_3\text{Cl}_2]$ with ZnMe_2 results in a remarkable series of C–H and P–C bond activation, as well as P–C and C–C bond formation, steps to generate $[\text{Ru}(\text{dppbz})(\text{PPh}_2(\text{biphenyl}))(\text{ZnMe})]$ (**1**; dppbz = 1,2-bis(diphenylphosphino)benzene; $\text{PPh}_2(\text{biphenyl})$ = cyclometallated $\text{PPh}_2(\text{biphenyl})$). The order of these transformations on the pathway to formation of the chelating diphenylphosphino-benzene and cyclometallated (diphenylphosphino)biphenyl ligands has been probed by ^1H and ^{31}P NMR spectroscopy. Initial studies of the reactivity of **1** show that both H_2 and the C–H bond of an alkyne can add across the Ru–Zn bond, with reversal of $\text{Ph}_2\text{P}(\text{biphenyl})$ metalation also taking place.

Results and discussion

Characterisation of $[\text{Ru}(\text{dppbz})(\text{PPh}_2(\text{biphenyl}))\text{ZnMe}]$ (**1**) and trapping with CO

Treatment of $[\text{Ru}(\text{PPh}_3)_3\text{Cl}_2]$ with ZnMe_2 (5 equiv.)⁶ in THF led to the evolution of a single red product over 48 h, which was characterised as $[\text{Ru}(\text{dppbz})(\text{PPh}_2(\text{biphenyl}))\text{ZnMe}]$ (**1**, Scheme 2) arising from the remarkable transformation of two of the PPh_3 ligands into a bidentate bis(diphenylphosphino)benzene ligand, and conversion of the third PPh_3 into a (diphenylphosphino)biphenyl ligand, which undergoes cyclometallation at the ruthenium centre.⁷

Fig. 1 shows the X-ray structure of **1**. The geometry can be described as a distorted square pyramid based on maximum

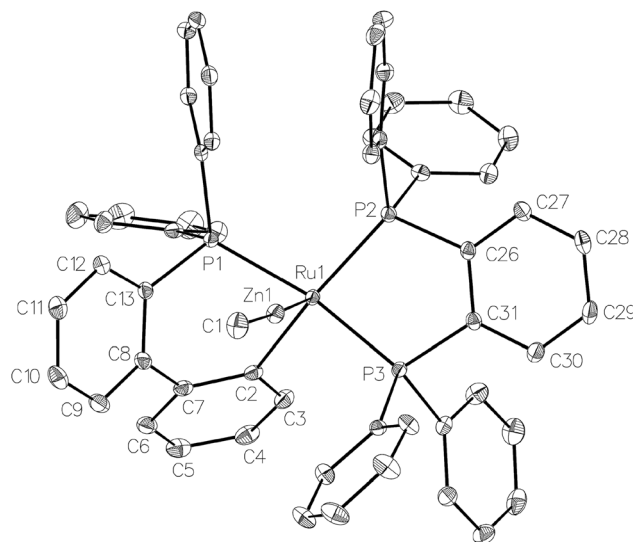
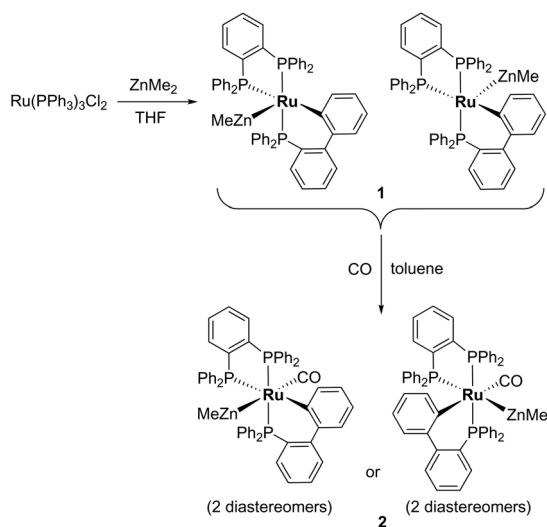


Fig. 1 Molecular structure of **1**. Ellipsoids are represented at 30% probability. Hydrogen atoms and guest solvent have been omitted for clarity.

deviations of +0.264 Å and –0.297 Å for P1 and C2, respectively, either side of the mean-plane containing atoms Ru1, P1, P2, P3 and C2. The apical position in the structure is occupied by the ZnMe ligand, which is *trans* to a vacant site.⁸ The Ru–Zn distance of 2.3713(3) Å is shorter than that in **A** (R = Me; 2.4069(7) Å), **D** (2.3997(8) Å) or **E** (2.3819(4) Å).³

Dissolution of **1** in C_6D_6 gave a $^{31}\text{P}\{^1\text{H}\}$ NMR spectrum (ESI ‡) comprising of two sets of three resonances in a 5:1 mixture, which were assigned as diastereomers (Scheme 2) by comparison to the results from the reaction of $[\text{Ru}(\text{BINAP})(\text{PPh}_3)\text{HCl}]$ with ZnMe_2 described below. The major isomer of **1** exhibited a doublet of doublets ($^2J_{\text{PP}} = 257$, 3 Hz) resonance at δ 65, assigned to one terminus of the dppbz ligand. The large $^2J_{\text{PP}}$ splitting of 257 Hz arises from coupling to the *trans*-cyclometallated $\text{PPh}_2(\text{biphenyl})$ ligand, which itself appeared as a doublet of doublets ($^2J_{\text{PP}} = 257$, 18 Hz) at δ 51.⁹ The small couplings of 18 and 3 Hz showed that both phosphorus nuclei were *cis* to the second terminus of the dppbz ligand, which appeared at δ 79. The minor diastereomer exhibited analogous signals at δ 78, 62 and 69 respectively, with similar sized coupling constants. Interconversion of the two diastereomers was shown by $^{31}\text{P}\{^1\text{H}\}$ EXSY measurements (ESI ‡).

Trapping of **1** by CO gave the coordinatively saturated carbonyl complex, $[\text{Ru}(\text{dppbz})(\text{PPh}_2(\text{biphenyl}))(\text{CO})\text{ZnMe}]$ (**2**, Scheme 2) in a rapid reaction that was accompanied by colour change from red to pale yellow. Complex **2** was characterised by a combination of NMR and IR data, but proved elusive to crystallographic characterisation. As in the case of **1**, **2** was present in solution as what we believe is a mixture of two diastereomers, in a ratio of *ca.* 1:1.3. The minor isomer appeared in the room temperature $^{31}\text{P}\{^1\text{H}\}$ NMR spectrum as two sharp, overlapping doublets at δ 67, with couplings of 243 and 18 Hz, and a sharp doublet of doublets at δ 47 ($^2J_{\text{PP}} = 243$, 18 Hz), whereas the major isomer displayed three very broad signals.



Scheme 2 Formation of $[\text{Ru}(\text{dppbz})(\text{PPh}_2(\text{biphenyl}))\text{ZnMe}]$ (**1**) and trapping by CO.



These resolved upon cooling to 223 K into a doublet of doublets at δ 75 ($^2J_{PP} = 241, 12$ Hz), a broad triplet at δ 59 and a second doublet of doublets at δ 46 ($^2J_{PP} = 241, 18$ Hz). The solution IR spectrum of **2** (in $C_6D_5CD_3$) showed a carbonyl stretch for each of the two isomers at 1934 cm^{-1} and 1911 cm^{-1} (ESI ‡).

When **1** was reacted with ^{13}CO , each of the ^{31}P resonances of $2\text{-}^{13}CO$ exhibited an additional doublet with a $^2J_{PC}$ splitting of 7–11 Hz (ESI ‡). A geometry in which all three phosphorus nuclei are *cis* to the carbonyl ligand is implied by the magnitude of these couplings, but the absence of an X-ray structure precluded us from being able to elucidate whether the $ZnMe$ was *trans* to CO or a phosphine (Scheme 2). In the $^{13}C\{^1H\}$ NMR spectrum of $2\text{-}^{13}CO$, the carbonyl resonance of the minor diastereomer appeared as a sharp quartet ($^2J_{CP} = 8$ Hz) at δ 204 at room temperature (this broadened upon cooling), whereas that of the major diastereomer only ever appeared as a broad resonance at δ 209, even down at 211 K.

Mechanism of formation of **1**

^{31}P NMR monitoring of the reaction of $[Ru(PPh_3)_3Cl_2]\cdot PPh_3$ and $ZnMe_2$ showed that the formation of **1** proceeded through two sets of intermediates (Fig. 2). One set formed very early in the reaction and was identified at low temperature by NMR spec-

troscopy. The second set appeared later in the reaction and proved amenable to room temperature spectroscopic scrutiny.

Characterisation of these two sets of intermediates (see below) led us to the mechanistic hypothesis depicted in Scheme 3. The initial addition of $ZnMe_2$ to $[Ru(PPh_3)_3Cl_2]\cdot PPh_3$ gives the 'early' intermediates **I–III**, which all feature two *ortho*-metallated PPh_3 ligands (step i). Further reaction with $ZnMe_2$, followed by C–C coupling,¹⁰ generates the late intermediates **IV–VI** (step ii) which contain 2,2'-bis(diphenylphosphino)biphenyl (BIPHEP) ligands. A formal P–C/Ru–C metathesis reaction¹¹ involving BIPHEP and $PPh_2(C_6H_4)$ ligands in step iii¹² ultimately yields **1**.¹³ Support for the formation of BIPHEP containing species on the mechanistic pathway was provided by the reaction of $ZnMe_2$ with an *in situ* generated sample of $[Ru(BIPHEP)(PPh_3)HCl]$ (Scheme 3, step iv) which produced NMR signals for **IV–VI**, as well as the final product **1** (ESI ‡).

Characterisation of intermediates **I–VI**

A low temperature (246 K) reaction of $ZnMe_2$ and $[Ru(PPh_3)_3Cl_2]\cdot PPh_3$ generated intermediates **I–III**, which appeared in the form of three very broad ^{31}P NMR signals at δ 51, –27 and –39. As shown in Fig. 3, these resolved into five low and four higher frequency resonances at 210 K. Intermediates **I–III** were assigned as bis-cyclometallated

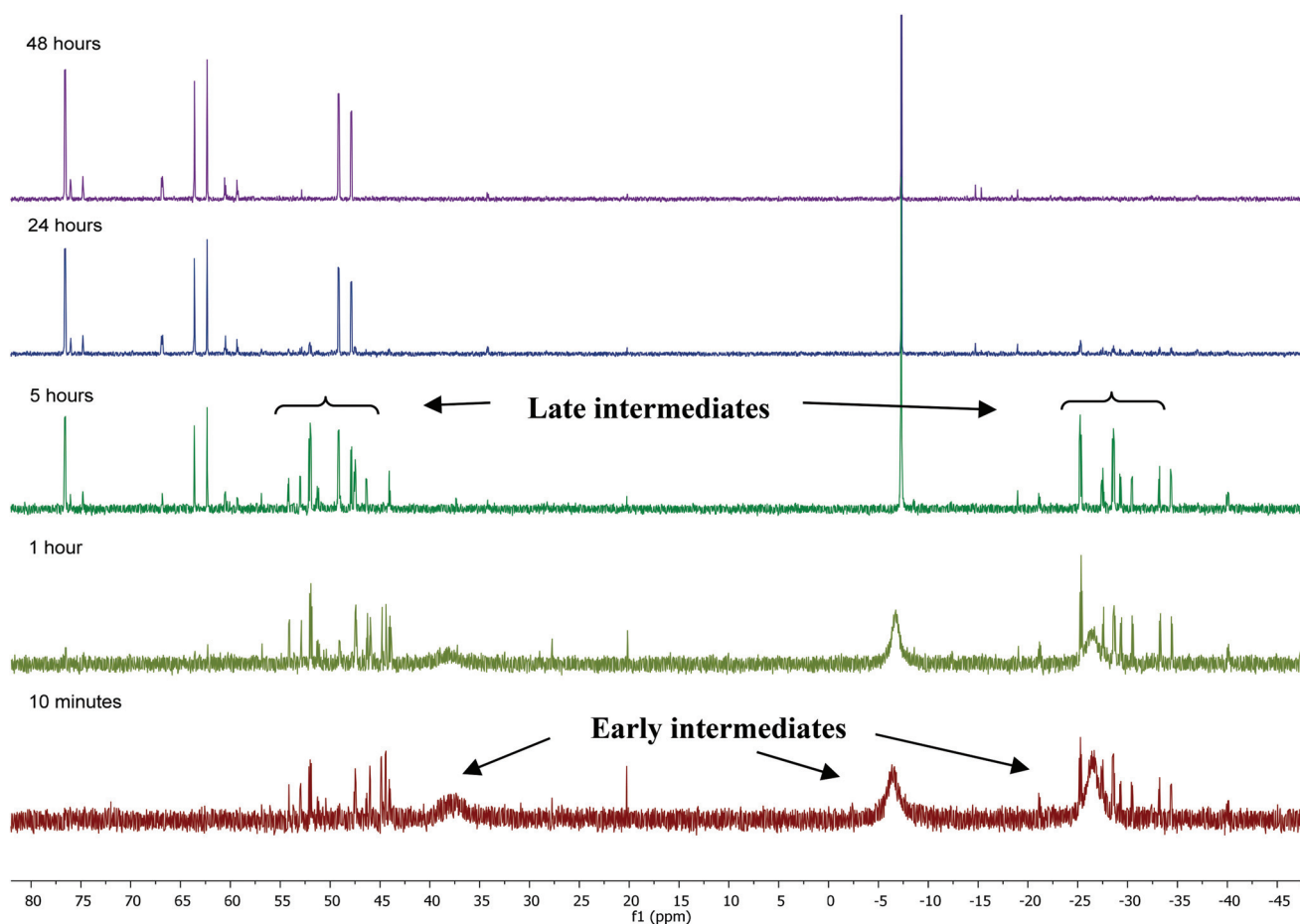
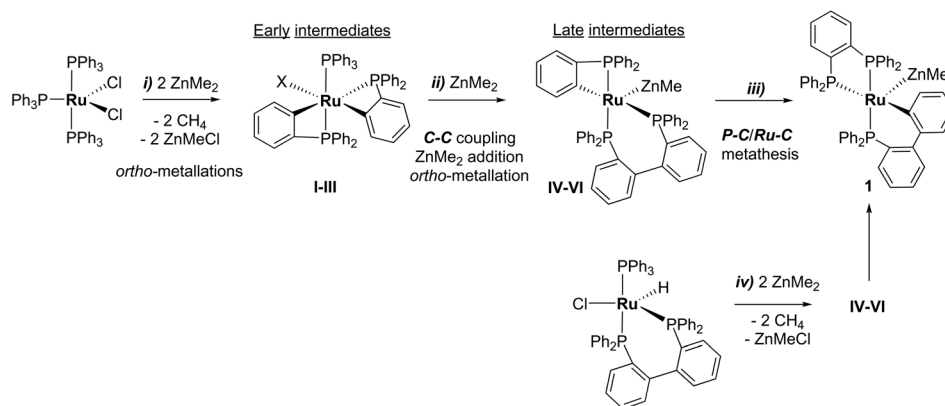
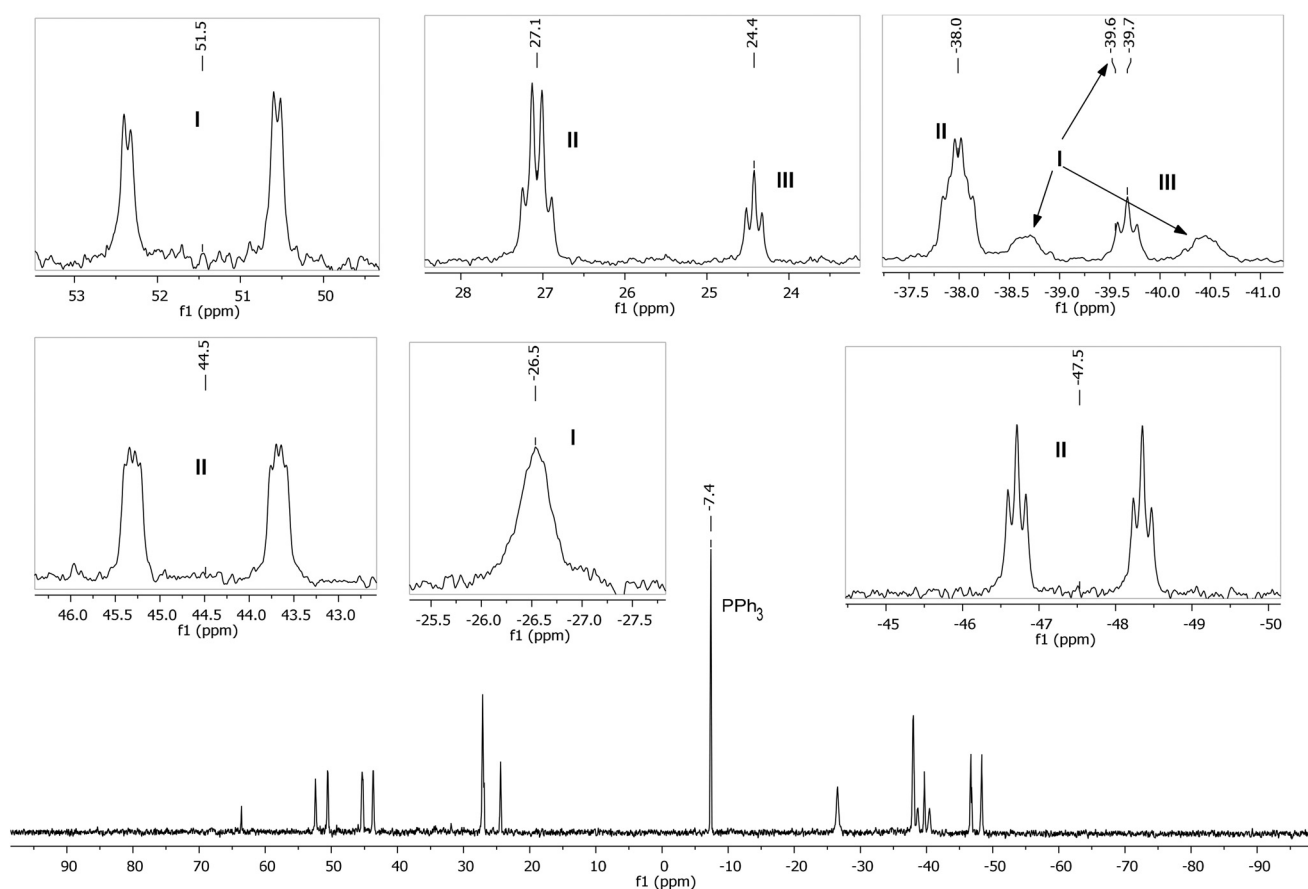


Fig. 2 $^{31}P\{^1H\}$ NMR spectra (202 MHz, $THF-d_8$, 298 K) showing the progress of the reaction between $[Ru(PPh_3)_3Cl_2]\cdot PPh_3$ and $ZnMe_2$ with time.

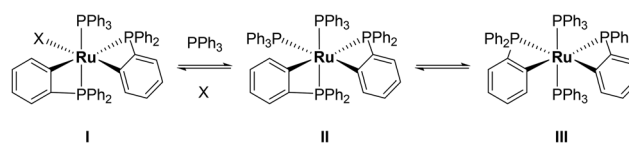




Scheme 3 Proposed mechanism for the formation of 1.

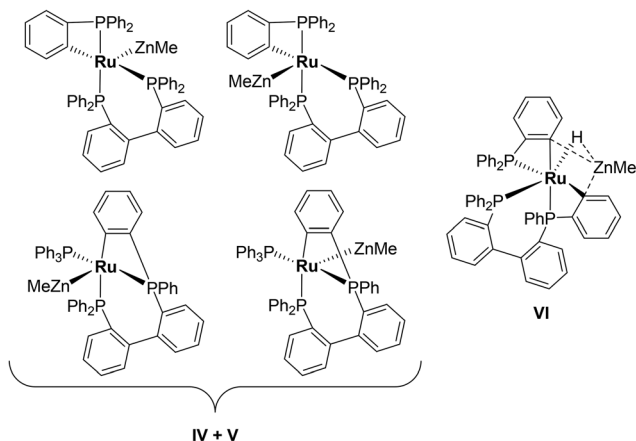
Fig. 3 Low temperature (210 K) $^{31}\text{P}\{^1\text{H}\}$ NMR spectrum (162 MHz, THF- d_6) showing intermediates I–III, with assignments and multiplicities indicated in the insets.

species (Scheme 4) based on the number of resonances, their chemical shifts (the low frequency signals are diagnostic of four-membered ring cyclometallated species)^{9,14} and ^{31}P COSY measurements (ESI†). Geometries were based upon the magnitudes of $^2J_{\text{PP}}$. The pale yellow colour of the reaction mixture (*cf.* the red colour of **1**) supports I–III being coordinatively satu-



Scheme 4 Proposed structure for intermediates I–III.

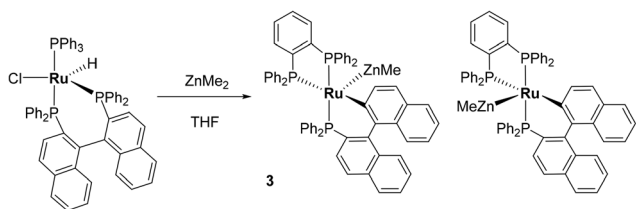




Scheme 5 Proposed structures for intermediates IV–VI.

rated, although the exact nature of the two-electron donor X in species **I** remains unknown; ZnMe_2 , ZnMeCl or THF are the most likely candidates.¹⁵ The intermediates **I–III** were present in a ratio of *ca.* 3.5 : 5.5 : 1 and were shown to be in exchange by $^{31}\text{P}\{^1\text{H}\}$ EXSY measurements.

The formation of a second set of intermediates **IV–VI** was established in a separate experiment in which a 1 : 5 molar



Scheme 6 Formation of $[\text{Ru}(\text{dppbz})(\text{PPh}_2(\text{binaphthyl}))\text{ZnMe}]$ (**3**).

ratio of $[\text{Ru}(\text{PPh}_3)_3\text{Cl}_2]\cdot\text{PPh}_3$ and ZnMe_2 were combined at room temperature. Tellingly, **IV** and **V** each showed just a single cyclometallated $^{31}\text{P}\{^1\text{H}\}$ NMR resonance, together with two other higher frequency signals (ESI†). We propose that **IV** and **V** must also contain ZnMe ligands in order to remain as $\text{Ru}(\text{II})$. Structures consistent with these data are shown in Scheme 5, although NMR spectra do not allow them to be differentiated. The identity of **VI** was more straightforward given the presence of one high and two low frequency $^{31}\text{P}\{^1\text{H}\}$ resonances, and a doublet of triplets hydride resonance ($\delta -8.05$ ppm, $^2J_{\text{HP}} = 46.8$ Hz, $^2J_{\text{HP}} = 13.4$ Hz; ESI†). **VI** is related to **IV** and **V** by an additional cyclometallation reaction. The proposed structures of the three intermediates were based upon a comparison of chemical shifts and coupling constants to triphenylphosphine derivatives formed in the reaction of $[\text{Ru}(\text{PPh}_3)_3\text{HCl}]$ with ZnMe_2 .⁵

Synthesis and characterisation of $[\text{Ru}(\text{dppbz})(\text{PPh}_2(\text{binaphthyl}))\text{ZnMe}]$ (**3**)

Given the reactivity of $[\text{Ru}(\text{BIPHEP})(\text{PPh}_3)\text{HCl}]$ (Scheme 3), ZnMe_2 was added to the racemic BINAP derivative $[\text{Ru}(\text{rac-BINAP})(\text{PPh}_3)\text{HCl}]$ (*rac*-BINAP = racemic-2,2'-bis(diphenylphosphino)-1,1'-binaphthyl).¹⁶ An instantaneous colour change from red-orange to deep green was observed,¹⁷ which reverted back to red upon heating at 70 °C (24 h). $^{31}\text{P}\{^1\text{H}\}$ NMR spectroscopy (ESI†) showed the presence of two new species in a 1 : 1 ratio, both of which exhibited three high frequency doublet of doublet resonances (δ 77, 69, 63; δ 79, 68, 53). The signals were assigned to two diastereomers (*vide infra* for crystallographic confirmation) of $[\text{Ru}(\text{dppbz})(\text{PPh}_2(\text{binaphthyl}))\text{ZnMe}]$ (**3**, Scheme 6). In contrast to **1**, the diastereomers did not exchange by ^{31}P EXSY (ESI†).

Compound **3** exhibited a broadly analogous structure to **1** (Fig. 4), in terms of the co-ordination geometry about the central ruthenium,^{18,19} however, the square based pyramid

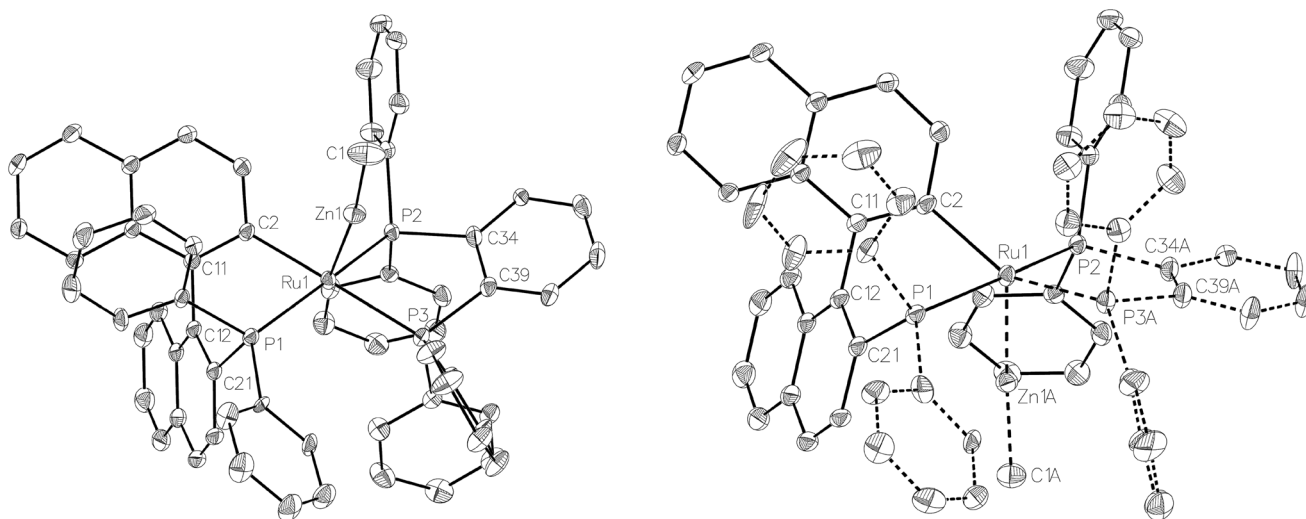


Fig. 4 Molecular structure of the two, mutually disordered, diastereomers present in the structure of **3**, from approximately similar viewpoints. Ellipsoids are represented at 30% probability. Hydrogen atoms and guest solvent have been omitted for clarity.



was substantially less distorted than that in **1**, as evidenced by maximum deviations of +0.17 Å and -0.087 Å for Ru1 and P3, respectively, either side of the mean-plane containing the ruthenium centre, the three P atoms and the cyclometallated carbon. The Ru–Zn distance was even further reduced in **3** compared to **1** (to 2.2867(6) Å), although the two Ru–C_{metallated} bond lengths were similar in both cases (**1**: 2.111(2) Å; **3**: 2.120(2) Å). Both of these values are noticeably longer than the equivalent metric of 2.051(4) Å reported for a cycloruthenated Cy₂P(binaphthyl)' ligand.¹⁸ The crystal structure of **3** was heavily disordered such that the asymmetric unit contains an overlay of two diastereomers (Fig. 4). The two components (53 : 47 occupancy ratios) are related by an approximate (non-crystallographic) mirror which bisects the P3–Ru1–P3A angle. As the disorder only impacts, in a minor way, on the asymmetric ligand that contains atom P1, the disordered fractions are not mirror images of each other.

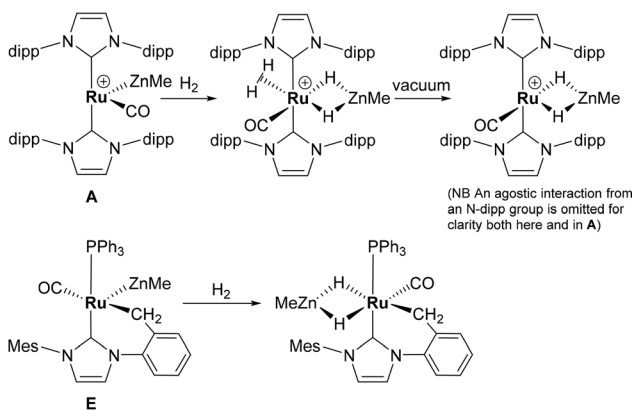
Reactivity of **1** with H₂ and PhC≡CH

The presence of both unsaturated Ru and Zn centres afforded an opportunity to compare the reactivity of **1** with that previously reported for **A** and **E** (summarised in Scheme 7).^{2,3,20}

The addition of 1 atm H₂ to a toluene-*d*₈ solution of **1** brought about an instantaneous change from the red colour of the coordinatively unsaturated starting material to colourless, again indicative of coordinatively saturated Ru. Three new broad, low frequency hydride resonances were present in the ¹H NMR spectrum of the reaction mixture. Cooling to 246 K partially resolved these signals and showed they were present in a 1 : 1 : 1 ratio (ESI[†]). Together with the ³¹P{¹H} resonances

(δ 86 (dd, ²J_{PP} = 242, 24 Hz), 81 (t, ²J_{PP} = 25 Hz), 58 (dd, ²J_{PP} = 242, 26 Hz); ESI[†]), these data are consistent with the formation of *mer*-[Ru(dppbz)(Ph₂P(biphenyl))(H)₂(H)(ZnMe)] (**4**), arising through a reaction with two equivalents of H₂. One equivalent added across the Ru–Zn bond to afford a Ru(H)₂Zn moiety, while the second added across the Ru–C bond to reverse the cyclometallation of the Ph₂P(biphenyl)' ligand, also generating a terminal Ru–H ligand in the process (Scheme 8).

Complex **1** also reacted with two molecules of PhC≡CH (Scheme 8) to form the structurally characterised *mer*-isomer of [Ru(dppbz)(Ph₂P(biphenyl))(C≡CPh)₂(H)(ZnMe)] (**5**). Compound **5** results from C–H activation of one equivalent of alkyne across the Ru–Zn bond,²¹ together with C–H activation of a second equivalent, leading to reversal of biphenyl group cyclometallation and generation of a terminal Ru-acetylide ligand. The X-ray structure (Fig. 5) revealed several features worthy of comment. The Zn atom was asymmetrically bound to the μ-η²:η¹-C≡CPh ligand, with Zn(1)–C(2) and Zn(1)–C(3) distances of 2.1123(17) Å and 2.4415(18) Å, respectively. These differences mirror what is seen in the few other examples of compounds in which there is an apparent side-on interaction involving zinc and a C≡C bond.^{22,23} Similarly, the interaction



Scheme 7 Summary of the reactions of [Ru(IPr₂(CO)ZnMe)⁺] and [Ru(IMes)(PPh₃)(CO)(ZnMe)] with H₂.

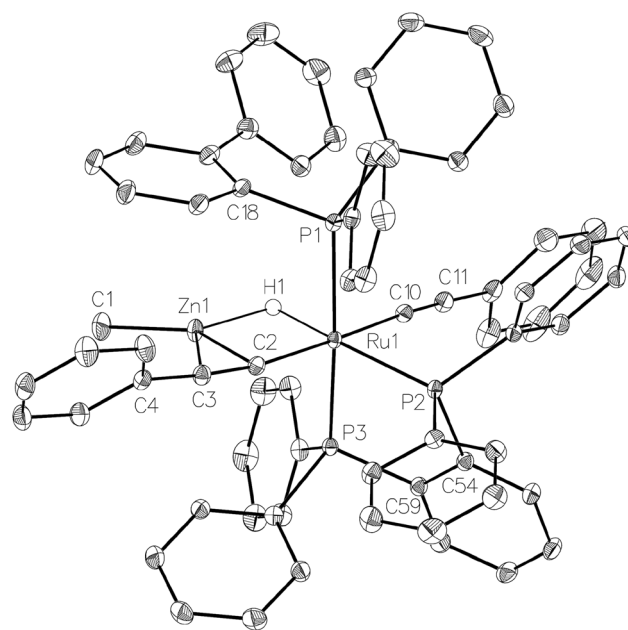
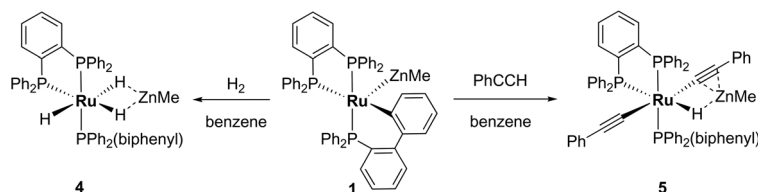


Fig. 5 Molecular structure of **5**. Ellipsoids are represented at 30% probability. Guest solvent and hydrogen atoms, with the exception of H1, have been omitted for clarity.



Scheme 8 Reactivity of **1** with H₂ and PhC≡CH.



with zinc led to a slightly less linear Ru–C≡C unit (167.83°) than in the terminal acetylide ligand (175.11°). The two C≡C distances were similar within 3σ. The presence of two different acetylide groups was also apparent from the presence of two C≡C vibrations (2082, 2012 cm⁻¹)²² in the IR spectrum.

Both **4** and **5** displayed only limited stability, slowly degrading over time in solution (**5** also slowly degraded in the solid-state) at room temperature.

Conclusions

In contrast to the ‘simple’ Ru–Zn products **A**, **D** and **E** (Scheme 1) which are formed upon addition of ZnMe₂ to [Ru(NHC)₂(CO)H]⁺ (NHC = IPr, IBiox) and [Ru(NHC)(PPh₃)(CO)HCl] (NHC = IMes), [Ru(PPh₃)₃Cl₂] reacts through a series of C–H activation, C–C coupling, P–C activation and P–C bond forming steps to give [Ru(dppbz)(PPh₂(biphenyl))(ZnMe)] (**1**). Although the individual reactions involved in the overall transformation of three PPh₃ ligands into Ph₂PC₆H₄PPh₂ and Ph₂P(biphenyl) groups have been observed separately,¹¹ to the best of our knowledge, there are no examples in which they have been observed in concert with one another. The role of ZnMe₂ is central to the observation of the chemistry, as it provides a means to bring about the elimination of both CH₄ and ZnMeCl, allowing access to highly reactive, low-valent ruthenium fragments capable of performing the array of bond activation/formation steps observed. Additional studies of novel Ru–Zn heterobimetallic complexes that highlight this even further will be reported in due course.

Experimental

All manipulations were carried out using standard Schlenk, high vacuum and glovebox techniques. Solvents were purified using an MBraun SPS solvent system (hexane, Et₂O) or under a nitrogen atmosphere from sodium benzophenone ketyl (benzene, THF). C₆D₆, toluene-*d*₈ and THF-*d*₈ were vacuum transferred from potassium. CD₂Cl₂ was dried over CaH₂. NMR spectra were recorded on Bruker Avance 400 and 500 NMR spectrometers at 298 K (unless stated otherwise) and referenced as follows; ¹H: chemical shifts of residual protio solvent resonances (C₆D₆ δ 7.16, THF-*d*₈ δ 3.58, CD₂Cl₂ δ 5.32, C₆D₅CD₃ δ 2.08); ¹³C{¹H}: solvent signal for C₆D₅CD₃ (δ 20.4); ³¹P{¹H}: externally to 85% H₃PO₄ (δ 0.0). IR spectra were recorded in C₆D₅CD₃ solution or in KBr discs on a Nicolet Nexus spectrometer. Elemental analyses were performed by Elemental Microanalysis Ltd, Okehampton, Devon, UK. Literature methods were used to prepare [Ru(PPh₃)₃Cl₂]-PPh₃,^{6a,24} [Ru(PPh₃)₃Cl₂],²⁴ and [Ru(PPh₃)₃HCl]-toluene.²⁵ Racemic [Ru(*rac*-BINAP)(PPh₃)HCl]-0.35BINAP was prepared by an analogous process to that described for [Ru(*R*-BINAP)(PPh₃)HCl].¹⁶

[Ru(dppbz)(PPh₂(biphenyl))(CO)ZnMe] (**1**)

ZnMe₂ (1.25 mL of 2.0 M toluene solution, 2.5 mmol) was added to a THF (25 mL) suspension of [Ru(PPh₃)₃Cl₂]-PPh₃

(610 mg, 0.5 mmol) and the mixture stirred for 42 h. After removal of the solvent and residual ZnMe₂ under vacuum, the red residue was redissolved in THF (10 mL), filtered and the filtrate layered with hexane (14 mL). A red crystalline solid was collected, washed with Et₂O (6 mL) and dried under vacuum. Yield: 230 mg (48%). Employing [Ru(PPh₃)₃Cl₂] as the precursor gave 236 mg of the title product as a red solid (49% yield). **1** exists in solution as an equilibrium mixture of 2 diastereomers in a 5:1 ratio (referred to as *maj* and *min* below). ¹H NMR: δ_H (500 MHz, C₆D₆) 7.71–7.62 (m, 1H_{*maj*}, 1H_{*min*}, Ar), 7.62–7.53 (m, 5H_{*maj*}, 5H_{*min*}, Ar), 7.51–7.19 (m, 9H_{*maj*}, 9H_{*min*}, Ar), 7.12–6.71 (m, 24H_{*maj*}, 26H_{*min*}, Ar), 6.68 (t, *J* = 7.5 Hz, 2H_{*maj*}, Ar), 6.62 (t, *J* = 7.3 Hz, 1H_{*maj*}, Ar), 6.34 (t, *J* = 7.2 Hz, 1H_{*min*}, Ar), 0.08 (s, 3H_{*min*}, ZnCH₃), -1.00 (s, 3H_{*maj*}, ZnCH₃). ³¹P{¹H} NMR: δ_P (202 MHz, C₆D₆) 79.1 (dd, ²*J*_{PP} = 18, 3 Hz, dppbz_{*maj*}), 77.6 (dd, ²*J*_{PP} = 250, 7 Hz, dppbz_{*min*}), 68.9 (dd, ²*J*_{PP} = 18, 7 Hz, dppbz_{*min*}), 65.3 (dd, ²*J*_{PP} = 257, 3 Hz, dppbz_{*maj*}), 62.0 (dd, ²*J*_{PP} = 250, 18 Hz, PPh₂(biphenyl)_{*min*}), 50.6 (dd, ²*J*_{PP} = 257, 18 Hz, PPh₂(biphenyl)_{*maj*}). Anal. Calcd for C₅₅H₄₅P₃ZnRu: C, 68.43, H, 4.70%; Found: C, 67.89, H, 4.84%.

[Ru(dppbz)(PPh₂(biphenyl))(CO)ZnMe] (**2**)

A J. Young's resealable NMR tube was charged with **1** (10 mg, 0.01 mmol) in C₆D₅CD₃ (0.5 mL), and placed under 1 atm CO (or ¹³CO). Vigorous shaking brought about a colour change from deep red to pale yellow and complete dissolution of starting material was achieved within a few minutes. The solution was analysed by ¹H and ³¹P{¹H} NMR spectroscopy, which showed that **2** was present as a mixture of 2 diastereomers in a ratio of *ca.* 1.3:1 (referred to as *maj* and *min* below). Selected ¹H NMR: δ_H (400 MHz, C₆D₅CD₃, 223 K) -0.52 (s, ZnCH₃_{*maj*}), -1.54 (s, ZnCH₃_{*min*}). ³¹P{¹H} NMR: δ_P (162 MHz, C₆D₅CD₃, 223 K) 75.0 (dd, ²*J*_{PP} = 241, 12 Hz, dppbz_{*maj*}), 68.1 (d, ²*J*_{PP} = 18 Hz, dppbz_{*min*}), 68.0 (d, ²*J*_{PP} = 241 Hz, dppbz_{*min*}), 58.7 (t, ²*J*_{PP} = 15 Hz, dppbz_{*maj*}), 48.6 (dd, ²*J*_{PP} = 241, 18 Hz, PPh₂(biphenyl)_{*min*}), 46.3 (dd, ²*J*_{PP} = 241, 18 Hz, PPh₂(biphenyl)_{*maj*}). ²⁻¹³CO: Selected ¹³C{¹H} NMR: δ_C (101 MHz, C₆D₅CD₃, 223 K) 208.7 (m, RuCO_{*maj*}), 203.9 (q, ²*J*_{PC} = 8 Hz, RuCO_{*min*}). ³¹P{¹H} NMR: δ_P (162 MHz, C₆D₅CD₃, 223 K) 75.0 (dt, ²*J*_{PP} = 242, 11 Hz, ²*J*_{PC} = 11 Hz, dppbz_{*maj*}), 68.1 (dd, ²*J*_{PP} = 18 Hz, ²*J*_{PC} = 7 Hz, dppbz_{*min*}), 68.0 (dd, ²*J*_{PP} = 241 Hz, ²*J*_{PC} = 7 Hz, dppbz_{*min*}), 58.7 (m, dppbz_{*maj*}), 48.6 (ddd, ²*J*_{PP} = 241, 18 Hz, ²*J*_{PC} = 8 Hz, PPh₂(biphenyl)_{*min*}), 46.3 (ddd, ²*J*_{PP} = 242, 18 Hz, ²*J*_{PC} = 11 Hz, PPh₂(biphenyl)_{*maj*}). IR (C₆D₅CD₃, cm⁻¹): 1934 (ν_{CO}), 1911 (ν_{CO}).

Detection and characterisation of intermediates I–III

ZnMe₂ (42 μL of 1.2 M toluene solution, 0.05 mmol) in THF-*d*₈ (0.2 mL) was vacuum transferred into a J. Young's resealable NMR tube containing a THF-*d*₈ (0.3 mL) solution of [Ru(PPh₃)₃Cl₂]-PPh₃ (12 mg, 0.01 mmol). The solution was maintained at <200 K prior to insertion into a pre-cooled (210 K) NMR spectrometer. After warming to 246 K for 15 min to initiate reaction, the temperature was returned to 210 K to prevent further reaction and ¹H, ³¹P{¹H}, ³¹P COSY and ³¹P EXSY measurements of intermediates **I–III** recorded. The



reaction mixture was then warmed to room temperature. After 8 h, $^{31}\text{P}\{^1\text{H}\}$ NMR spectroscopy revealed the formation of intermediates **IV–VI** (see below), as well as the final product **1**. $^{31}\text{P}\{^1\text{H}\}$ NMR of **I**: δ_{P} (162 MHz, THF- d_8 , 210 K) 51.5 (dd, $^2J_{\text{PP}} = 292$, 14 Hz), -26.5 (br s), -39.6 (br d, $^2J_{\text{PP}} = 290$ Hz). $^{31}\text{P}\{^1\text{H}\}$ NMR of **II**: δ_{P} (162 MHz, THF- d_8 , 210 K) 44.5 (ddd, $^2J_{\text{PP}} = 265$, 18, 9 Hz), 27.1 (q, $^2J_{\text{PP}} = 19$ Hz), -38.0 (td, $^2J_{\text{PP}} = 19$, 10 Hz), -47.5 (dt, $^2J_{\text{PP}} = 266$, 19 Hz). $^{31}\text{P}\{^1\text{H}\}$ of **III**: δ_{P} (162 MHz, THF- d_8 , 210 K) 24.4 (t, $^2J_{\text{PP}} = 16$ Hz), -39.7 (t, $^2J_{\text{PP}} = 16$ Hz).

Detection and characterisation of intermediates of **IV–VI**

A J. Young's resealable NMR tube was charged with $[\text{Ru}(\text{PPh}_3)_3\text{Cl}_2]\cdot\text{PPh}_3$ (12 mg, 0.01 mmol) in THF- d_8 (0.5 mL) and ZnMe_2 (42 μL of 1.2 M toluene solution, 0.05 mmol) was added. After standing for 3.5 h at room temperature, ^1H , $^{31}\text{P}\{^1\text{H}\}$, ^{31}P HMQC and ^{31}P COSY measurements were used to characterise the three intermediates **IV–VI**. $^{31}\text{P}\{^1\text{H}\}$ NMR of **IV**: δ_{P} (202 MHz, THF- d_8) 55.4 (dd, $^2J_{\text{PP}} = 240$, 15 Hz), δ 49.4 (dd, $^2J_{\text{PP}} = 20$, 15 Hz), -31.9 (dd, $^2J_{\text{PP}} = 240$, 20 Hz). $^{31}\text{P}\{^1\text{H}\}$ NMR of **V**: δ_{P} (202 MHz, THF- d_8) 48.8 (dd, $^2J_{\text{PP}} = 234$, 18 Hz), 45.9 (dd, $^2J_{\text{PP}} = 22$, 18 Hz), -28.0 (dd, $^2J_{\text{PP}} = 234$, 22 Hz). Selected ^1H NMR of **VI**: δ_{H} (500 MHz, THF- d_8) -8.05 (dt, $^2J_{\text{HP}} = 46.8$, 13.4 Hz, 1H, RuH). $^{31}\text{P}\{^1\text{H}\}$ NMR of **VI**: δ_{P} (202 MHz, THF- d_8) δ 53.9 (dd, $^2J_{\text{PP}} = 24$, 21 Hz), -23.4 (dd, $^2J_{\text{PP}} = 21$, 19 Hz), -26.7 (dd, $^2J_{\text{PP}} = 24$, 19 Hz).

Reaction of $[\text{Ru}(\text{BIPHEP})(\text{PPh}_3)\text{HCl}]$ and ZnMe_2

$[\text{Ru}(\text{BIPHEP})(\text{PPh}_3)\text{HCl}]$ was prepared *in situ* upon heating (40 $^\circ\text{C}$, 24 h) $[\text{Ru}(\text{PPh}_3)_3\text{HCl}]\cdot\text{toluene}$ (10 mg, 0.01 mmol) and BIPHEP (5 mg, 0.01 mmol) in CD_2Cl_2 (0.6 mL). The resulting red-orange solution comprised *ca.* 80% $[\text{Ru}(\text{BIPHEP})(\text{PPh}_3)\text{HCl}]$, together with $[\text{Ru}(\text{PPh}_3)_3\text{HCl}]$ (*ca.* 12%) and a third species attributed to $[\text{Ru}(\text{BIPHEP})_2\text{HCl}]$ (*ca.* 8%). After removal of solvent, the red residue was redissolved in THF- d_8 (0.5 mL) and ZnMe_2 (42 μL of 1.2 M toluene solution, 0.05 mmol) added. A $^{31}\text{P}\{^1\text{H}\}$ NMR spectrum recorded 6 h later showed the presence of intermediates **IV–VI**, along with **1**. Selected ^1H NMR of $[\text{Ru}(\text{BIPHEP})(\text{PPh}_3)\text{HCl}]$: δ_{H} (500 MHz, CD_2Cl_2) -22.78 (dt, $^2J_{\text{HP}} = 37$, 23 Hz, 1H, RuH). $^{31}\text{P}\{^1\text{H}\}$ NMR of $[\text{Ru}(\text{BIPHEP})(\text{PPh}_3)\text{HCl}]$: δ_{P} (202 MHz, CD_2Cl_2) 87.0 (dd, $^2J_{\text{PP}} = 38$, 21 Hz), 41.2 (dd, $^2J_{\text{PP}} = 305$, 38 Hz), 35.5 (dd, $^2J_{\text{PP}} = 305$, 21 Hz). Selected ^1H NMR of $[\text{Ru}(\text{BIPHEP})_2\text{HCl}]$: δ_{H} (500 MHz, CD_2Cl_2) -16.47 (tt, $^2J_{\text{HP}} = 24$, 15 Hz, 1H, RuH). $^{31}\text{P}\{^1\text{H}\}$ NMR of $[\text{Ru}(\text{BIPHEP})_2\text{HCl}]$: δ_{P} (202 MHz, CD_2Cl_2) 35.8 (t, $^2J_{\text{PP}} = 35$ Hz), 22.2 (t, $^2J_{\text{PP}} = 35$ Hz).

$[\text{Ru}(\text{dppbz})(\text{PPh}_2(\text{binaphthyl}))\text{ZnMe}]$ (**3**)

ZnMe_2 (0.50 mL of 1.2 M toluene solution, 0.6 mmol) was added to a THF (6 mL) suspension of racemic $[\text{Ru}(\text{rac-BINAP})(\text{PPh}_3)\text{HCl}]\cdot 0.35\text{BINAP}$ (120 mg, 0.10 mmol), leading to an immediate colour change from red-orange to deep green. The solution was then heated for 24 h at 70 $^\circ\text{C}$. After removal of the solvent, the red residue was redissolved in THF (1.5 mL), filtered through a pad of Celite® and the filtrate treated with hexane (3 mL). After standing for 24 h, free BINAP was separated by filtration through Celite® and a further 1 mL hexane

added to the filtrate to give, over 24 h, a red crystalline solid, which was isolated and dried under vacuum. Yield: 58 mg, *ca.* 90% pure (49% yield). A sample of the product (20 mg) was recrystallised from THF/hexane to give 15 mg of pure material. **3** exists as a mixture of two diastereomers (referred to as *A* and *B* below) in a ratio of *ca.* 1:1 ratio. These were assigned by comparison with the NMR signals of minor and major diastereomers of **1**. ^1H NMR: δ_{H} (500 MHz, C_6D_6) 7.96 (d, $J = 8.5$ Hz, 1H, Ar), 7.82 (t, $J = 8.5$ Hz, 2H, Ar), 7.73–7.34 (m, 25H, Ar), 7.33–7.18 (m, 5H, Ar), 7.15–6.82 (m, 39H, Ar), 6.81–6.68 (m, 10H, Ar), 6.67–6.49 (m, 8H, Ar), 6.23 (t, $J = 7.1$ Hz, 2H, Ar), 0.15 (s, 3H_A, ZnCH_3), -1.40 (s, 3H_B, ZnCH_3). $^{31}\text{P}\{^1\text{H}\}$ NMR: δ_{P} (202 MHz, C_6D_6) 78.5 (dd, $^2J_{\text{PP}} = 18$, 3 Hz, dppbz_B), 77.1 (dd, $^2J_{\text{PP}} = 248$, 11 Hz, dppbz_A), 68.6 (dd, $^2J_{\text{PP}} = 17$, 11 Hz, dppbz_A), 68.2 (dd, $^2J_{\text{PP}} = 255$, 3 Hz, dppbz_B), 63.4 (dd, $^2J_{\text{PP}} = 248$, 17 Hz, $\text{PPh}_2(\text{binaphthyl})_{\text{A}}$), 52.8 (dd, $^2J_{\text{PP}} = 255$, 18 Hz, $\text{PPh}_2(\text{binaphthyl})_{\text{B}}$). Anal. Calcd for $\text{C}_{63}\text{H}_{49}\text{P}_3\text{ZnRu}$: C, 71.02; H, 4.64%; Found: C, 71.25; H, 5.05%.

$[\text{Ru}(\text{dppbz})(\text{Ph}_2\text{P}(\text{biphenyl}))(\text{H})_2(\text{H})(\text{ZnMe})]$ (**4**)

A J. Young's resealable NMR tube was charged with **1** (10 mg, 0.01 mmol) in $\text{C}_6\text{D}_5\text{CD}_3$ (0.5 mL) and placed under 1 atm H_2 . Vigorous shaking brought about a colour change from deep red to pale yellow. Complete dissolution of starting material took place in <10 min. The resulting fine suspension was filtered through a pad of Celite® and rapidly (<30 min) analysed by ^1H and $^{31}\text{P}\{^1\text{H}\}$ NMR spectroscopy, which showed clean formation of **4**. Slow decomposition of the product took place in solution at room temperature, precluding isolation. ^1H NMR: δ_{H} (400 MHz, $\text{C}_6\text{D}_5\text{CD}_3$, 246 K) 8.54 (t, $J = 9.0$ Hz, 2H, Ar), 8.15 (dd, $J = 12.5$, 8.2 Hz, 1H, Ar), 7.99 (t, 8.5 Hz, 2H, Ar), 7.57–7.37 (m, 6H, Ar), 7.36–6.92 (m, 16H, Ar; overlapped with residual solvent signals in $\text{C}_6\text{D}_5\text{CD}_3$), 6.91–6.80 (m, 6H, Ar), 6.79–6.65 (m, 8H, Ar), 6.59 (t, $J = 7.2$ Hz, 2H, Ar), -0.89 (s, 3H, ZnCH_3), -7.08 (quint, $^2J_{\text{HP}} = 8.9$ Hz, 1H, RuH), -8.37 (dt, $^2J_{\text{HP}} = 52.1$ Hz, 19.4 Hz, 1H, RuH), -8.62 (m, 1H, RuH). $^{31}\text{P}\{^1\text{H}\}$ NMR: δ_{P} (162 MHz, $\text{C}_6\text{D}_5\text{CD}_3$, 246 K) 85.5 (dd, $^2J_{\text{PP}} = 242$, 24 Hz), 81.2 (t, $^2J_{\text{PP}} = 25$ Hz), 57.9 (dd, $^2J_{\text{PP}} = 242$, 26 Hz).

$[\text{Ru}(\text{dppbz})(\text{Ph}_2\text{P}(\text{biphenyl}))(\text{C}\equiv\text{CPh})_2(\text{H})(\text{ZnMe})]$ (**5**)

A suspension of **1** (97 mg, 0.1 mmol) in C_6H_6 (2 mL) was treated with $\text{PhC}\equiv\text{CH}$ (33 μL , 0.3 mmol) and the mixture stirred vigorously for 3 h. The resulting yellow fine suspension was filtered through a pad of Celite®, diluted with hexane (7.5 mL) and crystallized at -35 $^\circ\text{C}$. Yellow crystalline solid was separated, washed with hexane (1.5 mL \times 2) and dried under vacuum. Yield: 106 mg (90%). The product undergoes slow decomposition both in solution and in the solid-state at room temperature. ^1H NMR: δ_{H} (500 MHz, C_6D_6) 8.76 (dd, $J = 13.8$, 8.0 Hz, 1H, Ar), 8.62 (t, $J = 9.1$ Hz, 2H, Ar), 8.20 (br t, $J = 8.3$ Hz, 2H, Ar), 7.66 (t, $J = 7.3$ Hz, 1H, Ar), 7.57 (t, $J = 7.6$ Hz, 1H, Ar), 7.44–7.29 (m, 6H, Ar), 7.22 (d, $J = 7.4$ Hz, 2H, Ar), 7.19–6.60 (m, 38H, Ar), -0.47 (s, 3H, ZnCH_3), -6.91 (dt, $^2J_{\text{HP}} = 59.6$, 16.2 Hz, 1H, RuH). $^{31}\text{P}\{^1\text{H}\}$ NMR: δ_{P} (202 MHz, C_6D_6) 73.8 (dd, $^2J_{\text{PP}} = 275$, 20 Hz), 55.8 (dd, $^2J_{\text{PP}} = 24$, 20 Hz), 37.9 (dd, $^2J_{\text{PP}} = 275$, 24 Hz). IR (KBr, cm^{-1}): 2082 ($\nu\text{C}\equiv\text{C}$), 2012 ($\nu\text{C}\equiv\text{C}$). Anal.



Calcd for $C_{71}H_{57}P_3ZnRu$: C, 72.91; H, 4.91%; Found: C, 73.03; H, 4.89%.

X-ray crystallography

Data for **1** were collected on an Agilent Xcalibur diffractometer (using Mo-K α radiation) while those for **3** and **5** were obtained using an Agilent SuperNova instrument and a Cu-K α source. All experiments were conducted at 150 K. Using Olex2,²⁶ all structures were solved with the olex2.solve²⁷ structure solution program and subsequently refined using the SHELXL program.²⁸

Points of note include the fact that the asymmetric unit in **1** contains a portion of solvent in addition to one molecule of the complex. While the former was identifiable as a hexane moiety, the disorder was so extensive that modelling would have resulted in excessive parameterization. Hence, the solvent was treated using the solvent mask in Olex2. However, the formula as presented, herein, accounts for the presence of a 1 : 1 ratio of the title compound to hexane in the crystal.

The asymmetric unit in **3** resolved beautifully, once the rampant disorder was addressed. In particular, Zn1, P3, the methyl group based on C1 and the phenyl groups based on C34, C40, C41, C45 and C58 were all treated for 53 : 47 disorder. Some distance and ADP restraints were included in the model (on merit), in disordered regions – to assist convergence. There was also a modicum of disordered solvent in the asymmetric unit, which did not lend itself to being readily modelled. As above, this was treated with the solvent mask algorithm available in Olex2, and an allowance for one molecule of THF per unit cell has been made in the formula as presented – to account for the pre-squeeze electron density evident in the difference Fourier electron density map. It merits note that strenuous checks were performed regarding the diffraction pattern symmetry in this structure, given the level of disorder present. Integration of the data in the triclinic, reduced cell [$a = 10.8687(3)$, $b = 12.1871(3)$, $c = 20.5157(5)$ Å, $\alpha = 79.451(2)$, $\beta = 81.396(2)$, $\gamma = 80.252(2)^\circ$] afforded two molecules in the asymmetric unit (as expected) in $P1$ plus some solvent. Both of the complex molecules exhibited similar disorder to that presented for the $Pbca$ solution/refinement reported herein. Ultimately, the exercise of testing in space-group $P1$ served as reassurance that the evident disorder is real. H1 in the structure of **5** was located and refined freely. Three guest molecules of benzene were also found in the asymmetric unit for this crystal.

Crystallographic data for all compounds have been deposited with the Cambridge Crystallographic Data Centre as supplementary publications CCDC 1937663–1937665 for **1**, **3** and **5**, respectively.

Conflicts of interest

There are no conflicts of interest to declare.

Acknowledgements

We thank the EU (Marie Curie Individual Fellowship to FMM (792674 H2020-MSCA-IF 2017)) for financial support.

References

- For reviews, see: (a) *Molecular Metal-Metal Bonds: Compounds, Synthesis, Properties*, ed. S. T. Liddle, Wiley-VCH, Weinheim, 2015; (b) A. Maity and T. S. Teets, *Chem. Rev.*, 2016, **116**, 8873–8911. For specific examples, see: (c) F. N. Tebbe, *J. Am. Chem. Soc.*, 1973, **95**, 5412–5414; (d) J. N. St. Denis, W. Butler, M. D. Glick and J. P. Oliver, *J. Organomet. Chem.*, 1977, **129**, 1–16; (e) P. H. M. Budzelaar, A. A. H. Vanderzeijden, J. Boersma, G. J. M. Vanderkerk, A. L. Spek and A. J. M. Duisenberg, *Organometallics*, 1984, **3**, 159–163; (f) J. W. Bruno, J. C. Huffman and K. G. Caulton, *J. Am. Chem. Soc.*, 1984, **106**, 444–445; (g) D. L. Thorn and R. L. Harlow, *J. Am. Chem. Soc.*, 1989, **111**, 2575–2580; (h) M. D. Fryzuk, D. H. McConville and S. J. Rettig, *Organometallics*, 1990, **9**, 1359–1360; (i) M. D. Fryzuk, D. H. McConville and S. J. Rettig, *Organometallics*, 1993, **12**, 2152–2161; (j) J. T. Golden, T. H. Peterson, P. L. Holland, R. G. Bergman and R. A. Andersen, *J. Am. Chem. Soc.*, 1998, **120**, 223–224; (k) R. A. Fischer, D. Weiss, M. Winter, I. Müller, H. D. Kaesz, N. Frölich and G. Frenking, *J. Organomet. Chem.*, 2004, **689**, 4611–4623; (l) M. Ohashi, K. Matsubara and H. Suzuki, *Organometallics*, 2007, **26**, 2330–2339; (m) C. J. Durango-García, J. O. C. Jiménez-Halla, M. López-Cardoso, V. Montiel-Palma, M. A. Muñoz-Hernández and G. Merino, *Dalton Trans.*, 2010, **39**, 10588–10589.
- I. M. Riddlestone, N. A. Rajabi, J. P. Lowe, M. F. Mahon, S. A. Macgregor and M. K. Whittlesey, *J. Am. Chem. Soc.*, 2016, **138**, 11081–11084.
- M. Espinal-Viguri, V. Varela-Izquierdo, F. M. Miloserdov, I. M. Riddlestone, M. F. Mahon and M. K. Whittlesey, *Dalton Trans.*, 2019, **48**, 4176–4189.
- I. M. Riddlestone, N. A. Rajabi, S. A. Macgregor, M. F. Mahon and M. K. Whittlesey, *Chem. – Eur. J.*, 2018, **24**, 1732–1738.
- F. M. Miloserdov, N. A. Rajabi, J. P. Lowe, M. F. Mahon, S. A. Macgregor and M. K. Whittlesey, unpublished results.
- (a) Both forms of $[Ru(PPh_3)_3Cl_2]$ (*i.e.* with and without co-crystallized PPh_3) could be utilized for the reaction and gave the same yield of **1**. H. Samouei, F. M. Miloserdov, E. C. Escudero-Adan and V. V. Grushin, *Organometallics*, 2014, **33**, 7279–7283; (b) The overall reaction requires 3 equivalents of $ZnMe_2$; 2 equivalents to abstract chloride in the form of $ZnMeCl$, and the third to provide the $ZnMe$ ligand in the product. An excess (5 equivalents) of $ZnMe_2$ was typically employed to drive the formation of **1** to completion.
- The formation of **1** contrasts markedly with the outcome of the reaction of $[Ru(PPh_3)_3Cl_2]$ and $AlMe_3$ in arene solvents



- which yields $[(\eta^6\text{-arene})\text{Ru}(\text{PPh}_3)_2\text{Me}][\text{AlCl}_2\text{Me}_2]$ salts as the products. X. G. Fang, J. G. Watkin, B. L. Scott, K. D. John and G. J. Kubas, *Organometallics*, 2002, **21**, 2336–2339.
- 8 C. J. Pell, W. C. Shih, S. Gatard and O. V. Ozerov, *Chem. Commun.*, 2017, **53**, 6456–6459.
- 9 (a) P. E. Garrou, *Inorg. Chem.*, 1975, **14**, 1435–1439; (b) P. E. Garrou, *Chem. Rev.*, 1981, **81**, 229–266.
- 10 P. A. Shaw, G. J. Clarkson and J. P. Rourke, *Chem. Sci.*, 2017, **8**, 5547–5558.
- 11 Y. H. Lee and B. Morandi, *Coord. Chem. Rev.*, 2019, **386**, 96–118.
- 12 (a) L. M. Alcazar-Roman, J. F. Hartwig, A. L. Rheingold, L. M. Liable-Sands and I. A. Guzei, *J. Am. Chem. Soc.*, 2000, **122**, 4618–4630; (b) S. Z. Ge, R. A. Green and J. F. Hartwig, *J. Am. Chem. Soc.*, 2017, **139**, 3300–3300.
- 13 Such a process can be mediated by transition metal phosphido complexes. P. E. Suess, A. J. Lough and R. H. Morris, *J. Am. Chem. Soc.*, 2014, **136**, 4746–4760.
- 14 F. Mohr, S. H. Priver, S. K. Bhargava and M. A. Bennett, *Coord. Chem. Rev.*, 2006, **250**, 1851–1888.
- 15 We envisage ZnMe_2 or ZnMeCl coordinating in $\text{Ru}\cdots\text{Zn}$ complexes in which Me and/or Cl groups bridge the two metal centres (ref. 5).
- 16 K. Abdur-Rashid, A. J. Lough and R. H. Morris, *Organometallics*, 2001, **20**, 1047–1049.
- 17 Studies to elucidate the structure of the initially formed green complex are ongoing and will be the subject of a subsequent publication.
- 18 N. Feiken, P. S. Pregosin, G. Trabesinger and M. Scalone, *Organometallics*, 1997, **16**, 537–543.
- 19 For other examples of P–C activation in $\text{Ru}(\text{BINAP})$ complexes, see: (a) T. J. Geldbach, P. S. Pregosin, A. Albinati and F. Rominger, *Organometallics*, 2001, **20**, 1932–1938; (b) T. J. Geldbach and P. S. Pregosin, *Eur. J. Inorg. Chem.*, 2002, 1907–1918; (c) T. J. Geldbach, P. S. Pregosin and A. Albinati, *Organometallics*, 2003, **22**, 1443–1451; (d) T. J. Geldbach, F. Breher, V. Gramlich, P. G. A. Kumar and P. S. Pregosin, *Inorg. Chem.*, 2004, **43**, 1920–1928.
- 20 IBiox complex **D** decomposes upon addition of H_2 (ref. 3).
- 21 For recent examples of alkyne C–H addition across Pt–Au/Ag bonds, see: (a) J. Campos, *J. Am. Chem. Soc.*, 2017, **139**, 2944–2947; (b) N. Hidalgo, C. Maya and J. Campos, *Chem. Commun.*, 2019, **55**, 8812–8815.
- 22 H. Lang, N. Mansilla and G. Rheinwald, *Organometallics*, 2001, **20**, 1592–1596.
- 23 E. E. Wilson, A. G. Oliver, R. P. Hughes and B. L. Ashfeld, *Organometallics*, 2011, **30**, 5214–5221.
- 24 P. S. Hallman, T. A. Stephenson and G. Wilkinson, *Inorg. Synth.*, 1970, **12**, 237–238.
- 25 R. A. Schunn, E. R. Wonchoba and G. Wilkinson, *Inorg. Synth.*, 1972, **13**, 131–134.
- 26 O. V. Dolomanov, L. J. Bourhis, R. J. Gildea, J. A. K. Howard and H. Puschmann, *J. Appl. Crystallogr.*, 2009, **42**, 339–341.
- 27 L. J. Bourhis, O. V. Dolomanov, R. J. Gildea, J. A. K. Howard and H. Puschmann, *Acta Crystallogr., Sect. A: Found. Adv.*, 2015, **71**, 59–75.
- 28 G. M. Sheldrick, *Acta Crystallogr., Sect. A: Found. Crystallogr.*, 1990, **46**, 467–473; G. M. Sheldrick, *SHELXL-97, a computer program for crystal structure refinement*, University of Göttingen, 1997.

